Anatomy Dependent Multi-Context Fuzzy Clustering for Separation of Brain Tissues in MR Images

CZ Zhu, FC Lin, TZ Jiang

National Laboratory of Pattern Recognition, Institute of Automation, Chinese Academy of Sciences, Beijing 100080, P.R. China
{czzhu, fclin, jiangtz}@nlpr.ia.ac.cn

Abstract. In a previous work, a local tissue distribution model and multi-context fuzzy clustering (MCFC) method had been proposed to successfully classify 3D T1-weighted MR images into tissues of white matter, gray matter, and cerebral spinal fluid in the condition of intensity inhomogeneities. This paper presents a complementary and improved version of MCFC. Firstly, quantitative analyses are added to validate the soundness of basic assumptions for MCFC. Carefully studies on the experiment results of MCFC on a set of simulated MR data disclose a fact that misclassification rate in a context of MCFC is spatially dependent on the anatomical position of the context; moreover, most of the misclassifications concentrate in regions of brain stem and cerebellum. Such unique distribution pattern of misclassification inspires us to choose different context size at such special anatomical regions. This anatomy-dependent MCFC (adMCFC) has been tested on both simulated and 10 clinical T1-weighted images and the experiments results show that adMCFC outperforms MCFC and other related methods.

1 Introduction

In general, white matter (WM), gray matter (GM) and cerebral spinal fluid (CSF), are three basic tissues in the brain. Brain tissue segmentation of MR images means to identify the tissue type for each point in data set on the basis of information available from both MR images and neuroanatomical knowledge. It is an important preprocessing step in many medical research and clinical applications, such as quantification of GM reduction in neurological and mental diseases, cortex segmentation and analysis, detection of pathology, surgical planning and navigation, multi-modality fusion and registration, functional brain mapping [1,2]. Unfortunately, intensity inhomogeneities, caused by both imperfections in imaging devices and biophysical properties variations in each tissue class, result in different MR signal intensities for the same tissue class at different locations in the brain. Hence intensity inhomogeneities are major obstacles to any intensity based automatic segmentation methods and have been investigated extensively [3, 4, 5, 6]. In one of our previous works, a local tissue distribution model and multi-context fuzzy clustering (MCFC) method for MRI brain tissue separation had been proposed [7] in order to eliminate or alleviate their adverse

impact. In this paper, anatomy dependent MCFC (adMCFC) is proposed to refine and improve the original MCFC.

The local tissue distribution model and MCFC method are briefly summarized in Section 2. adMCFC is presented in Section 3 followed by experimental results on both real and simulated 3-D MR data. The final section is devoted to discussion and conclusions.

2 Original MCFC Method

Clustering context is a key concept for the local tissue distribution model and MCFC. It is formally defined as a spatially connected subset of 3-D MRI brain volume corresponding to a specific region in the brain. The size of a context is defined as the number of pixels in the subset. The highly convoluted spatial distribution among different tissues in human brain inspires us to propose the local tissue distribution (LTD) model. LTD model consists of two assumptions:

(1) In any properly small context, three classes of tissues exist simultaneously and each with considerable proportion.

(2) In any properly small context, all pixels belonging to same tissue class will take on similar ideal signal intensities.

LTD model as well as the usual assumption that intensity inhomogeneities caused by imaging devices is smooth and slowly varying over the whole image domain constructed the foundation of MCFC. The following quantitative analyses are added here as a complementary explanation to validate the soundness of assumption (1) and (2). The simulated T1-weighted data as well as the corresponding labeled brain from the McConnell Brain Imaging Center at the Montreal Neurological Institute, McGill University [8] are used through the paper. Firstly, we proposed index of fractional anisotropy (FA) to describe the difference in proportions of three tissue classes in a given context.

$$FA = \frac{\sqrt{3} \cdot \sqrt{(n_w - \overline{n})^2 + (n_g - \overline{n})^2 + (n_s - \overline{n})^2}}{\sqrt{2} \cdot \sqrt{n_w^2 + n_g^2 + n_s^2}} \tag{1}$$

Where n_w, n_g, n_s is the number of pixels belonging to WM, GM, and CSF in a context respectively and $\overline{n}$ is the average number. Given context size, N contexts or brain regions are uniformly sampled in the labeled images and the averaged FA (aFA) among N contexts is treated as the measure of proportion difference for the given normalized context size (NCS) [7]. When three tissues have the same number pixels in a context then aFA reaches zero as the minimum, and aFA will increase with the number difference becomes more significant. aFA is plotted as a function of the context size in Fig. 1. From Fig. 1, we can see that aFA or difference in proportions of three tissue classes is decreasing when the context become larger. So if the context size is bigger enough then assumption (1) could be well guaranteed. As for assumption (2), we calculated the center of ideal signal distributions (CISD) for both WM

and GM in each context with given context size sampled from the 3-D simulated T1-weighted data without any noise and intensity inhomogeneities setting. CISD of each context can be plotted as the function of context position in the brain and GM CISD profiles are plotted in Fig 3 (a) ~ (d) corresponding to normalized context sizes of 0.02, 0.06, 0.10 and 0.18 respectively.

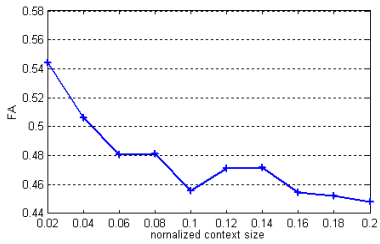

Fig. 1 FA distribution with NCS

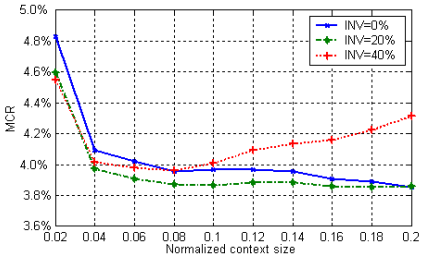

Fig. 2 MCR distribution with NCS

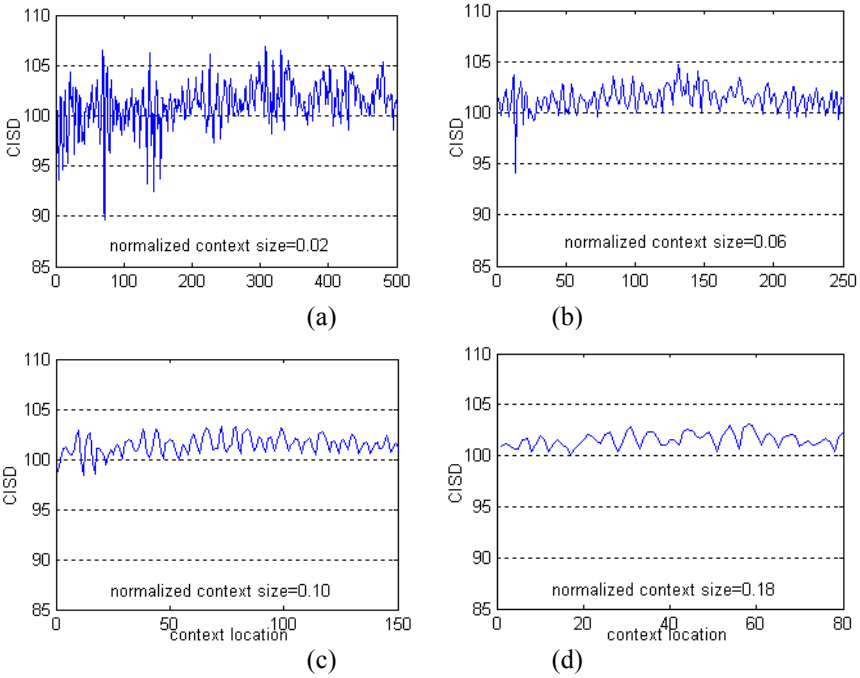

Fig. 3. CISD distribution of GM with context position in the brain, NCS= 0.02(a); 0.06 (b); 0.10 (c) and 0.18 (d)

We can see that CISD are quite different in different brain regions, especially for small context size, which indicates the impact of intensity inhomogeneities caused by biophysical properties variations in GM. Moreover, such difference will gradually decreased when the context size become larger to confuse signal distributions from different GM structures. Accordingly the assumption (2) required the context small enough. It is conflictive to choose context size for assumption (1) and assumption (2) simultaneously. The misclassification rate (MCR) of MCFC on simulated data set with 3% noise and 0%, 20% and 40% intensity inhomogeneities are plotted as the

function of normalized context size (NCS) in Fig.2. We can see that 0.06 is a tradeoff between both sides and can yield satisfying results.

Given a proper context size, MCFC includes two basic stages: multi-context fuzzy clustering and information fusion. In the first stage, multiple clustering contexts are generated for each pixel and fuzzy clustering is independently performed in each context on the basis of local imaging model to calculate the membership of the point to each tissue class. From the viewpoint of information fusion theory, the clustering contexts of a point can be regarded as information sources in the problem of tissue class determination, and intensity distributions in contexts are information provided by the sources. Here, the memberships can be regarded as soft decisions made upon the information from each information source independently. In the stage of information fusion, all the soft decisions are collected and integrated with some strategy in order to bias the final membership functions towards the majority results. And so the adverse impact from minority could be submerged by all the good clustering results from other contexts. Details about the implementation of MCFC and context size setting can be found in [7].

3 Anatomy-dependent MCFC

A carefully studies on the MCR of each context result in an interesting finding that MCR would vary in context at different position in the brain and most of the errors concentrate in the area of brain stem and cerebella as shown in Fig. 4. Moreover, the finding seems similar for the all three data sets.

Quantitatively analysis in FA suggests that higher FA makes assumption (1) not well guaranteed, which is, at least, part of the reason to concentrated misclassification in such area. We enlarge the context in these regions by multiplying the context size with an enlarging coefficient and calculated FA in the enlarged contexts. As shown in Fig. 5, averaged FA of contexts in such area decreases with the enlarging coefficient, which means we can make assumption (1) more correct by enlarging the context. In practice, a binary volume was created as the mask to identify the anatomic area to enlarge context as shown in Fig. 4.

The method of adMCFC can be summarized as follows:

(1) Find the anatomic area to enlarge the context in the target data a by a rigid registration process from the template to the target.

(2) Perform MCFC with a given context size. During context window moving through the target image, context center is tested to see whether it locates in such anatomical area or not. If yes, then enlarge the context by multiplying the context size with a given enlarging coefficient; If not, keep original context size.

It's very important for adMCFC to set a proper enlarging coefficient. Given normalized context size = 0.06 as we do in [7], three MCR curves are plotted as the function of the enlarging coefficient in Fig. 6 for simulated T1-weighted MRI data with 3% noise and 0%, 20% and 40% intensity inhomogenieties respectively. We can see that when enlarging coefficient is set between 1 and 4, the MCR will becomes smaller for all the intensity inhomogenieties conditions and moreover, the best classification result occurs at slightly different enlarging coefficients for the three intensity inho-

mogenieties conditions. In this work, we choose enlarging coefficients = 3 in all experiments.

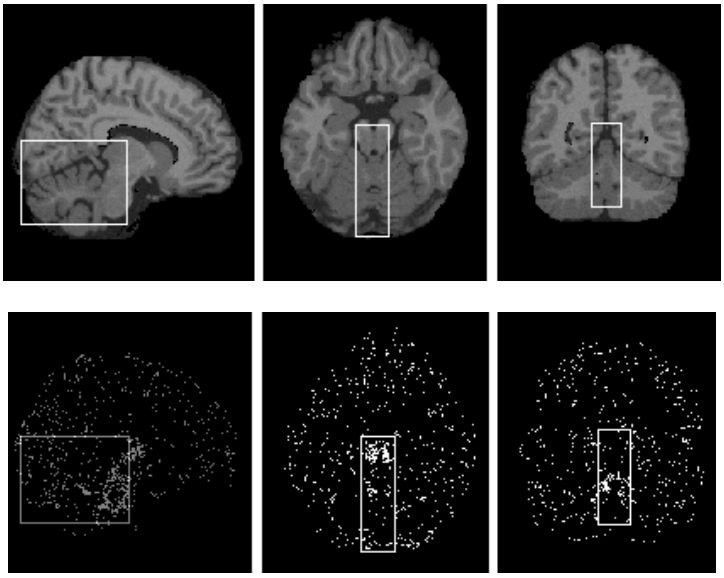

Fig.4 Original simulated T1-weighted MR data and the misclassified pixels. Box indicates the area with concentrated misclassification.

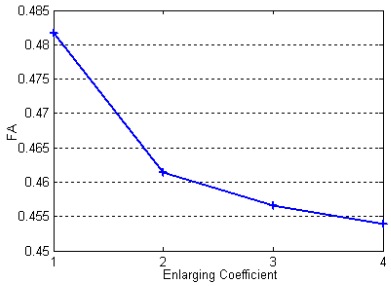

Fig. 5. FA and enlarging coefficient

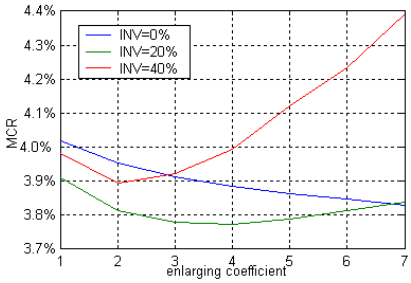

Fig. 6 MCR and enlarging coefficient

4 Experiments

4.1 Evaluation with 3-D simulated MRI data

In order to quantitatively evaluate the performance of adMCFC, adMCFC as well as MCFC and other related methods are tested on the same simulated MR data as in [7] and the results are listed in Table 1. We can see that both adMCFC and MCFC are significantly robust to increased inhomogeneities than FCM and FM-AFCM in [9].

Moreover, MCR of adMCFC is slower than that of MCFC in each intensity inhomogeneities level. Additionally, that adMCFC outperforms MCFC in the masked area can visually demonstrated in Fig.7. We can see that the misclassification pixels are obviously reduced.

Table 1. MCR from simulated data

Method	INV=0%	INV=20%	INV=40%
FCM	4.020%	5.440%	9.000%
FM-AFCM	4.168%	4.322%	4.938%
MCFC	4.020%	3.909%	3.979%
adMCFC	3.915%	3.780%	3.922%

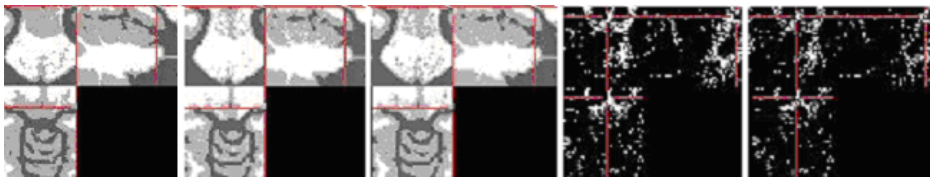

(a) (b) (c) (d) (e)

Fig. 7. Segmentation results. (a) True model (b) MCFC result (c) adMCFC result (d) MCFC misclassification (e) adMCFC misclassification

4.2 Evaluation with real T1-weighted MRI data

T1-weighted MRI data of 10 normal subjects (SIEMENS 1.5T, image size: $256 \times 256 \times 128$, resolution: $1.17\text{mm} \times 1.17\text{mm} \times 1.25\text{mm}$) are used to validate adMCFC. Fig. 8 shows the results from both adMCFC and FCM on the MR image of one of the 10 subjects. The intensity inhomogenieties and corresponding misclassifications can be easily detected at the top part in the original MR image and segmentation results of FCM. But adMCFC yields a much better result. Such improvement can also be demonstrated with 3D rendering of the segmented WM in Fig 9 where WM loss is very significant at the top area in the results of FCM.

5 Discussions and Conclusion

In this work we have qualitatively described the requirements of our local tissue distribution model and presented a improved MCFC method to separated brain tissue in T1-weighted MR images with more accuracy than MCFC as well as other related methods in the condition of intensity inhomogeneities. It is difficult for a fixed context size to guarantee the assumptions of LTD in all contexts because of the complexity in the brain. While adMCFC can determine the size of a context according to its anatomic position in the brain to result in lower misclassification rate than original MCFC can.

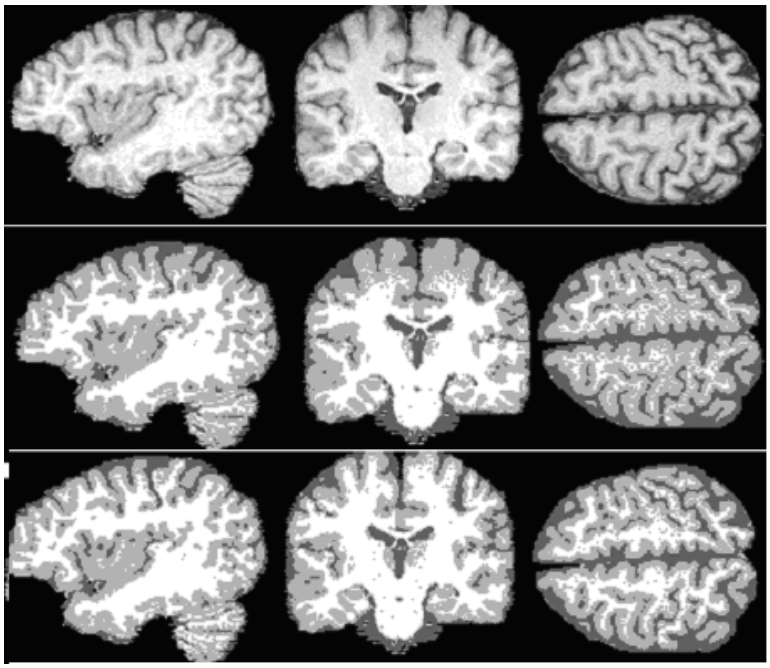

Fig. 8. Segmentation results. Original images (first row); FCM results (second row) and adMCFC results (third row)

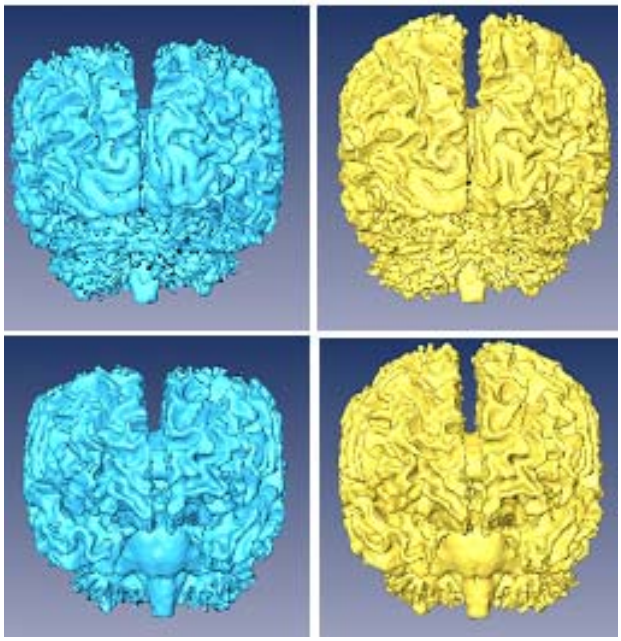

Fig. 9. 3D rendering of segmented WM from two view angles (top and bottom row). FCM results (left column) and adMCFC results (right column)

There are several issues to study further to improve the performance of adMCFC, such as the relationship between context size and enlarging coefficient, the shape and size of the mask to enlarge context. Please note that, we corrected a minor mistake in the MCFC algorithm so that we obtained slightly different results in Table 1 and Fig. 2 from those in [7].

References

1. Clarke, L. P., Velthuizen, R. P., Camacho, M. A., Heini, J. J., Vaidyanathan, M., Hall, L. O., Thatcher, R. W. and Silbiger, M. L. MRI Segmentation: Methods and Applications. Mag. Res. Imag. (1995) 13: 343-368.
2. Suri, J. S., Setarehdan, S. K. and Singh, S. Advanced Algorithmic Approaches to Medical Image Segmentation: state-of-the-art applications in cardiology, neurology, mammography and pathology. Spring-Verlag London Berlin Heidelberg, (2002).
3. Guillemaud, R. and Brady, M. Estimating the Bias Field of MR Images. IEEE Trans. Med. Imag. (1997). 16: 238-251.
4. Shattuck, D. W., Sandor-Leahy, S. R., Schaper, K. A., Rottenberg, D. A. and Leahy, R. M. Magnetic Resonance Image Tissue Classification Using a Partial Volume Model. Neuro-Image. (2001) 13: 856-876.
5. Worth, A. J., Markis, N., Caviness, V. S. and Kennedy, D. N. et al. Neuroanatomical segmentation in MRI: Technological Objectives. International J. of Pattern Recognition and Artificial Intelligent (1997) 11:1161-1187.
6. Arnold, J. B., Liow, J.-S., Schaper, K. A., et al. Qualitative and Quantitative Evaluation of Six Algorithms for Correcting Intensity Nonuniformity Effects. NeuroImage (2001) 13: 931–934.
7. C.Z. Zhu and T. Z. Jiang, "Multicontext fuzzy clustering for separation of brain tissues in magnetic resonance images", NeuroImage, Volume 18, Issue 3, (2003) Pages 685-696.
8. Collins, D. L., Zijdenbos, A. P., Kollokian, V., Sled, J. G.., Kabani, N.J., Holmes,C.J., Evans, A.C. Design and Construction of a Realistic Digital Brain Phantom. IEEE Trans. Med. Imag. (1998) 17: 463–468.
9. Pham, D. L. and Prince J. L. Adaptive Fuzzy Segmentation of Magnetic Resonance Images. IEEE Trans. Med. Imag. (1999) 18: 737-752.